

## Nonlinear dynamics of the hydrogen molecule

A. López-Castillo

*Centro de Ciências e Tecnologia (CCT), Departamento de Matemática, Universidade Federal de São Carlos (UFSCar),  
Caixa Postal 676, 13560-970, São Carlos, São Paulo, Brazil*

(Received 19 June 1997; revised manuscript received 7 April 1998)

The hydrogen molecule ( $H_2$ ) contains the basic ingredients for understanding the chemical bond, even more so than the hydrogen molecule ion.  $H_2$  is studied in the context of nonlinear dynamics. The classical mechanics of  $H_2$  is studied in three dimensions with nine, six, and three degrees of freedom and in one dimension (two degrees of freedom). The semiclassical quantization is made using the Bohr-Sommerfeld rules and the Gutzwiller formula to calculate the eigenvalues of the doubly occupied symmetric excited states of  $H_2$ . An *ab initio* quantum calculation is performed and compared with semiclassical results. The difficulties that appear in those calculations are discussed, and a proposal of the experimental measure is made.

[S1050-2947(98)05508-5]

PACS number(s): 31.10.+z, 03.20.+i, 05.45.+b, 31.25.-v

### I. INTRODUCTION

Bohr was the first to describe the electronic structure (chemical bond) from a physical point of view for a hydrogen molecule ( $H_2$ ) and other molecules [1,2]. Pauli tried to calculate the energy formation of the hydrogen molecule-ion ( $H_2^+$ ) by applying Bohr-Sommerfeld quantization [3]. However, correct procedures for the quantization were unknown [4]. With the advent of modern quantum mechanics, it was possible to calculate correctly the electronic structure for several molecules.

Calculations for one-electron molecules, e.g.,  $H_2^+$ , can be exactly solved (numerically) [5] by quantum mechanics in the Born-Oppenheimer approximation. For any molecule with two or more electrons in the same adiabatic approximation, it is not possible to know exactly the quantum solution, but sometimes it can be known with very high accuracy. In addition, the three-body (or unrestricted four-body) problem cannot be solved exactly by either quantum or classical theories. Nevertheless, the understanding of the electronic structure still presents several problems, because it is very difficult to understand quantum mechanics intuitively. The electronic structure of the ground state and the first excited states of the small molecules can be obtained with perfect accuracy by quantum mechanics depending on the computational sources. But it is very hard to obtain the quantum solution to the high excited state by an *ab initio* calculation, since there are enormous numerical convergence problems which demand a lot of computational time. Otherwise, limited quantum approximations must be used for this proposal.

Classical mechanics does not describe the electronic structure for quantum systems. However, it is a powerful technique to understand quantum mechanics. Following the old quantum theory, classical mechanics is implemented (correctly) with some added properties to describe quantum systems. This modified mechanics receives the name of semiclassical theory. It is an approximated theory which describes a system with increasing accuracy coupled with increasing excitation, i.e., when the quantum interference phenomenon becomes less important.

The semiclassical theory has recently become a very im-

portant technique, because it represents the connection between classical and quantum mechanics (the correspondence principle) for regular or chaotic systems. This connection can help “translate” quantum mechanics into classical terms. The understanding of this connection has a fundamental importance for the chemical bond [6,7] and for what occurs with chaos in the quantum world, when the analogous classical system is chaotic. To build the semiclassical mechanics of a system, it is necessary to know some classical properties such as periodic orbits and their magnitudes (period, action, etc.).

Classical mechanics can also be used to find adiabatic ways to solve the quantum problem. Some classical orbits described by several variables can present one variable that changes slowly in relation to the others. In this case, some adiabaticization can be done, and the slow variable can be taken as a parameter. The Born-Oppenheimer adiabaticization is the best known example of this. This adiabatic quantum calculation describes states close to those described by a corresponding classical orbit added by the semiclassical procedure. The application in the  $H_2^+$  system can be found in Refs. [3,4,8] for semiclassical quantization. Another example is the “frozen planetary atom” for helium [9,10].

Beyond the importance of giving the first step for the comprehension of the chemical bond, this study tries to recover the intuitive vision in the description of chemistry. For instance, it is necessary to include the electron exchange integrals, as it was done for the He atom [11], in a complete semiclassical treatment of the chemical bond of the  $H_2$ . That intuitive approach will not prevent a future development in quantum calculation, but can strongly influence the direction toward an understanding of some important chemical properties. The direct or indirect uses of classical mechanics in chemistry can mainly help studies of the excited states of complex systems.

This paper is a continuation and extension of a previous work on classical mechanics of  $H_2$  [6]. Here classical mechanics is studied under several approximations and degrees of freedom. There are many discussions about the semiclassical quantization and the quantum calculation. Of course, the semiclassical methods proposed here are considered as providing an additional, complementary understanding of the

chemical bond, but they are not an exclusive explanation of it.

The main objective of this paper is not only to develop a semiclassical procedure to describe the high excited states, but to obtain a description of states with few periodic orbits. The  $H_2$  system is an extremely complex problem from the point of view of the three-body problem (or restricted four-body problem) with six degrees of freedom; until today, to our knowledge, it has not been worked out. With a few simple orbits it is possible to simplify the problem, and thus the comprehension of the chemical bond can be improved. Atomic units are used throughout this paper unless otherwise specified.

## II. THEORY AND MODELS

The unrestrict four-body (nine degrees of freedom) Hamiltonian for  $H_2$  in Cartesian coordinates is presented below:

$$H_{H_2} = \frac{1}{2\mu} \mathbf{P}_R^2 + \frac{1}{2} (\mathbf{P}_1^2 + \mathbf{P}_2^2) - \frac{Z_A}{|\mathbf{r}_{1A}|} - \frac{Z_B}{|\mathbf{r}_{1B}|} - \frac{Z_A}{|\mathbf{r}_{2A}|} - \frac{Z_B}{|\mathbf{r}_{2B}|} + \frac{Z_A Z_B}{|\mathbf{R}|} + \frac{1}{|\mathbf{r}_2 - \mathbf{r}_1|}, \quad (1)$$

where  $\mu$  is the reduced mass of the nuclei,  $\mathbf{R}$  is the internuclear position vector,  $\mathbf{P}_R$  is the conjugate nuclear relative momentum vector,  $\mathbf{r}_i$  is the  $i$ th electron position vector,  $\mathbf{P}_i$  is the conjugate electronic momentum vector,  $\mathbf{r}_{iC}$  ( $= \mathbf{r}_i \pm \mathbf{R}/2$ ) is the  $i$ th electron position vector with respect to nuclei  $C$ , and  $Z_C$  ( $= 1$ , for  $H_2$ ) is the nuclear charge. In Eq. (1), the mass polarization term is avoided.

Equation (1) describes a Newtonian system, i.e., it is not connected to any electrodynamic phenomena. All comments made here about stabilities are related to Newtonian movements and not to electrodynamic ones. These are not considered here, since the ultimate objective is the quantization of the classical mechanics of the  $H_2$  system. In the same way, relativistic mechanics was included in neither classical nor quantum mechanics. Briefly, this work treats the nonintegrability and quantization of the Newtonian  $H_2$  multidimensional system.

Equation (1) can be reduced considering variable  $\mathbf{R}$  as a parameter. In this case, the system is reduced to six degrees of freedom (the restricted four-body problem).

The Hamiltonian [Eq. (1)] for adiabatic approximation can be written in the confocal elliptic coordinates defined by [12],  $\xi_i = (r_{iA} + r_{iB})/R$ ,  $\eta_i = (r_{iA} - r_{iB})/R$ , and  $\varphi_i$ , where  $\varphi_i$  is the azimuthal angle, and

$$H_{el} = \frac{2}{R^2(\xi_1^2 - \eta_1^2)} \left\{ (\xi_1^2 - 1)P_{\xi_1}^2 + (1 - \eta_1^2)P_{\eta_1}^2 + \left( \frac{1}{\xi_1^2 - 1} + \frac{1}{1 - \eta_1^2} \right) P_{\varphi_1}^2 \right\} - \frac{2}{R} \frac{(Z_A + Z_B)\xi_1 - (Z_A - Z_B)\eta_1}{(\xi_1^2 - \eta_1^2)} + \frac{2}{R^2(\xi_2^2 - \eta_2^2)} \left\{ (\xi_2^2 - 1)P_{\xi_2}^2 + (1 - \eta_2^2)P_{\eta_2}^2 + \left( \frac{1}{\xi_2^2 - 1} + \frac{1}{1 - \eta_2^2} \right) P_{\varphi_2}^2 \right\} - \frac{2}{R} \frac{(Z_A + Z_B)\xi_2 - (Z_A - Z_B)\eta_2}{(\xi_2^2 - \eta_2^2)} + \frac{2}{R} \{ (\xi_1^2 + \eta_1^2 - 1) + (\xi_2^2 + \eta_2^2 - 1) - 2\xi_1\xi_2\eta_1\eta_2 - 2\cos(\varphi_1 - \varphi_2)\sqrt{(\xi_1^2 - 1)(1 - \eta_1^2)(\xi_2^2 - 1)(1 - \eta_2^2)} \}^{-1/2}, \quad (2)$$

where  $H_{el}$  is the  $H_{H_2}$  adiabatic without the internuclear repulsion ( $Z_A Z_B/R$ ), and the subindices of the variables indicate the electrons.

This Hamiltonian [Eq. (2)] is singular, and is regularized [13] in order to eliminate the difficulties of the singularities which appear in the numerical calculation. The regularization procedure is made by expansion of the phase space. The time ( $t$ ) that describe the flux of Hamiltonian [Eq. (2)] and the energy ( $E$ ) are considered the canonical variables. The regularized Hamiltonian is given by

$$\Gamma = f(\xi_1, \eta_1, \xi_2, \eta_2)(H_{el} + P_t) = 0,$$

where  $f(\xi_1, \eta_1, \xi_2, \eta_2) = [(\xi_1^2 - \eta_1^2)(\xi_2^2 - \eta_2^2)/(\xi_1^2 \xi_2^2)]$  is a convenient function that vanishes with the singularities of Eq. (2),  $H_{el}$  is the same as in Eq. (2), and  $P_t \equiv -E$ . The new time ( $t'$ ) is defined by  $t' = f^{-1}(\xi_1, \eta_1, \xi_2, \eta_2)(t + \text{const})$ , the singularities are transferred to the time ( $t'$ ) and the integration becomes very slow in time ( $t$ ) near the singularities.

The canonical transformations are necessary to transform the  $\Gamma$  into canonical equation. The following variable transformations are made:

$$(2\chi_i/R)^2 = \xi_i^2 - 1,$$

$$\theta_i = \arccos \eta_i,$$

and the generating functions  $F_3(P_{\xi_i}, \chi_i) = -P_{\xi_i} [1 + (2\chi_i/R)^2]^{1/2}$  and  $F_3(P_{\eta_i}, \theta_i) = -P_{\eta_i} \cos \theta_i$  are required to calculate the conjugate momenta

$$P_{\chi_i} = (2/R)^2 \chi_i P_{\xi_i} / [1 + (2\chi_i/R)^2]^{1/2}$$

and

$$P_{\theta_i} = -P_{\eta_i} \sin \theta_i.$$

Finally, the regularized Hamiltonian is given by

$$\begin{aligned}
\Gamma = & \frac{1}{2} \frac{[\chi_2^2 + (R/2)^2 \sin^2 \theta_2]}{[\chi_2^2 + (R/2)^2]} P_{\chi_1}^2 + \frac{1}{2} \frac{[\chi_1^2 + (R/2)^2 \sin^2 \theta_1]}{[\chi_1^2 + (R/2)^2]} P_{\chi_2}^2 + \frac{1}{2} \frac{[\chi_2^2 + (R/2)^2 \sin^2 \theta_2]}{[\chi_1^2 + (R/2)^2][\chi_2^2 + (R/2)^2]} P_{\theta_1}^2 \\
& + \frac{1}{2} \frac{[\chi_1^2 + (R/2)^2 \sin^2 \theta_1]}{[\chi_1^2 + (R/2)^2][\chi_2^2 + (R/2)^2]} P_{\theta_2}^2 + \frac{[\chi_1^2 + (R/2)^2 \sin^2 \theta_1][\chi_2^2 + (R/2)^2 \sin^2 \theta_2]}{[\chi_1^2 + (R/2)^2][\chi_2^2 + (R/2)^2]} \\
& \times \left[ P_t + \frac{1}{2} \frac{P_{\varphi_1}^2}{\chi_1^2 \sin^2 \theta_1} + \frac{1}{2} \frac{P_{\varphi_2}^2}{\chi_2^2 \sin^2 \theta_2} \right] - \frac{[\chi_2^2 + (R/2)^2 \sin^2 \theta_2][(Z_A + Z_B)\sqrt{\chi_1^2 + (R/2)^2} - (Z_A - Z_B)(R/2)\cos \theta_1]}{[\chi_1^2 + (R/2)^2][\chi_2^2 + (R/2)^2]} \\
& - \frac{[\chi_1^2 + (R/2)^2 \sin^2 \theta_1][(Z_A + Z_B)\sqrt{\chi_2^2 + (R/2)^2} - (Z_A - Z_B)(R/2)\cos \theta_2]}{[\chi_1^2 + (R/2)^2][\chi_2^2 + (R/2)^2]} \\
& + \frac{[\chi_1^2 + (R/2)^2 \sin^2 \theta_1][\chi_2^2 + (R/2)^2 \sin^2 \theta_2]}{[\chi_1^2 + (R/2)^2][\chi_2^2 + (R/2)^2][R_{12}]}, \tag{3}
\end{aligned}$$

where

$$\begin{aligned}
R_{12} = & \{\chi_1^2 + \chi_2^2 + (R/2)^2(\cos^2 \theta_1 + \cos^2 \theta_2) \\
& - 2\sqrt{\chi_1^2 + (R/2)^2}\sqrt{\chi_2^2 + (R/2)^2} \cos \theta_1 \cos \theta_2 \\
& - 2 \cos(\varphi_1 - \varphi_2)\chi_1\chi_2 \sin \theta_1 \sin \theta_2\}^{1/2}.
\end{aligned}$$

The regularized Hamiltonian is transformed into the Hamiltonian of the helium atom in spherical coordinates for  $R=0$ . Equation (3) becomes similar to the pendulum Hamiltonian for one-electron systems (e.g.,  $H_2^+$ ) in the  $\chi \approx 0$  limit.

This Hamiltonian [Eq. (3)] is important to describe the  $H_2$  system completely. However, the one-dimensional (1D) approximation can be used, since the difficulties of the multi-dimensional calculation are drastically reduced.

The 1D Hamiltonian for  $H_2$  is given by

$$\begin{aligned}
H = & \frac{1}{2}(P_1^2 + P_2^2) - 1/|z_1 - R/2| - 1/|z_1 + R/2| - 1/|z_2 - R/2| \\
& - 1/|z_2 + R/2| + 1/|z_1 - z_2|, \tag{4}
\end{aligned}$$

where  $P_i$  is the momentum conjugated at position  $z_i$  of the electron. This Hamiltonian [Eq. (4)] is studied with both regularized and smoothed potentials. The smoothed potentials are given by

$$V_{\text{attr.}} = 1/[(z_i \pm R/2)^2 + \delta^2]^{1/2} \tag{5a}$$

and

$$V_{\text{rep.}} = 1/[(z_1 - z_2)^2 + \delta^2]^{1/2}, \tag{5b}$$

where  $V_{\text{attr.}}$  is the attraction potential between the proton and electron, and  $V_{\text{rep.}}$  is the interelectronic potential. The use of the regularized or smoothed potential shows different results for two (more)-electron system in the 1D model.

The regularized (1D) model has a centrifugal barrier over each nucleus that represents the true barrier in two dimensions [10]. That barrier implies a parabolic orbit ( $e=1$ , where  $e$  is the eccentricity) of the electrons around the nuclei. In this case, the  $H_2$  system divides the space into three regions separated by singular potentials. The smoothed potential (without barrier) connects the movements of electrons

(with enough energy) in these three regions. This connection will be discussed in the Sec. III.

The coupled Hamilton equations are obtained from the regularized or smoothed Hamiltonian and integrated numerically with the Runge-Kutta method of fifth order. The stability angles and the Lyapunov exponents of the periodic orbits can be obtained by the Monodromy method [14] as shown. The periodic orbit (PO) is a periodic solution of the Hamilton equation, and this solution is described by

$$\gamma_{\text{PO}}(T) = \gamma_{\text{PO}}(0),$$

where  $\gamma = (\mathbf{q}, \mathbf{p})$  and  $T$  is the period of the orbit. The  $[\gamma'(0) = \gamma_{\text{PO}} + \delta_{\gamma'}]$  initial condition is used to evaluate the neighborhood of the periodic orbit;  $\delta_{\gamma'}$  is a small displacement around periodic orbit. Using the  $[\gamma'(0)]$  in the Hamilton equations for one period, the  $[\gamma''(T) = \gamma_{\text{PO}} + \delta_{\gamma''}]$  result is obtained.

For the small displacement the following linear approximation is obtained:

$$\delta_{\gamma''} = \mathbf{M} \delta_{\gamma'},$$

where  $\mathbf{M}$  is the linear transformation matrix or monodromy matrix. The eigenvalues of  $\mathbf{M}$  are the stability angles (imaginary numbers) and the Lyapunov exponents (real numbers) for two degrees of freedom.

### III. RESULTS

#### A. Symmetric orbits and their stabilities

The symmetric orbits can be defined by the following coordinates:  $\xi_1 = \xi_2$ ,  $|\eta_1| = |\eta_2|$ ,  $|\cos(\varphi_1 - \varphi_2)| = 1$ ,  $P_{\xi_1} = P_{\xi_2}$ ,  $|P_{\eta_1}| = |P_{\eta_2}|$ , and  $|P_{\varphi_1}| = |P_{\varphi_2}|$  [see Eq. (2)]. It is possible to find various orbits for the  $H_2$  system starting from some known orbits for He [6,15,16]. A sketch of some orbits is presented in Fig. 1. Langmuir's orbits are obtained from Bohr's orbits by making a Bohr-Kramers' rotation ( $R_{\text{BK}}$ ) of the orbit of electron 1 over a plane conveniently selected. The main difference between the orbits in the He and  $H_2$  systems is the nonexistence of spherical symmetry in the  $H_2$ .

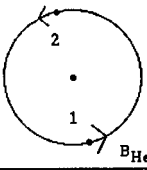
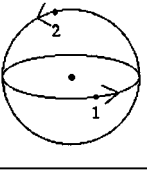
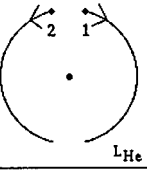
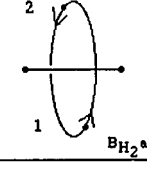
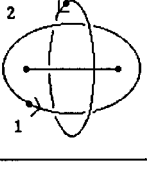
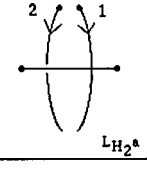
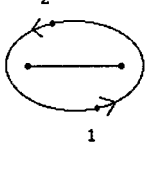
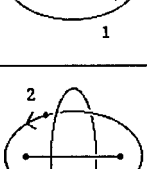
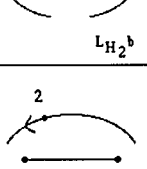
	Bohr	$R_{B-K}$	Langmuir
He			
H <sub>2</sub>			
			

FIG. 1. Bohr's and Langmuir's orbits for the helium atom (He) and for the hydrogen molecule (H<sub>2</sub>). Langmuir's orbits are obtained from Bohr's orbits by making a Bohr-Kramers rotation ( $R_{B-K}$ )

In the case of the H<sub>2</sub>, it is important to consider the system in three dimensions, since Bohr's and Langmuir orbits are different for  $R \neq 0$ .

These few orbits which appeared in Fig. 1 are considered here the most important ones to describe the multidimensional H<sub>2</sub> molecule. In the system with two degrees of freedom it is possible to find a great number of orbits systematically, although it is practically impossible to find them for higher degrees of freedom. Some insight about the orbits can be important in finding them, as in the Bohr and Langmuir orbits found for H<sub>2</sub> molecule.

Bohr proposed that the valence electrons (outer electrons) were located on a ring around the internuclear axis [ $B_{H_2}a$  orbit; see Fig. 1] representing the chemical bond [1,2,6]. The value of the chemical binding energy ( $E - 2E_H$ ) of the ground state ( $n=1$ ) agrees within 17% in relation to Langmuir's experimental value [2], where  $E$  is the total energy and  $E_H$  is the energy of the hydrogen atom in the ground state. In relation to modern measurements or quantum numerical calculations this error is around 6% for total energy, 41% in relation to chemical binding energy, and 21% for geometry. This is an acceptable result for the simple model that describes a complex system. The orbits that appear in Fig. 1 for the H<sub>2</sub> system are described in more details below and in Ref. [6].

The angular momentum for the  $B_{H_2}a$  orbit is constant as shown in Figs. 2(a) and 2(b) for 3D Cartesian space and momentum coordinates, respectively. Bohr made the angular momentum quantization of this particular orbit trying to

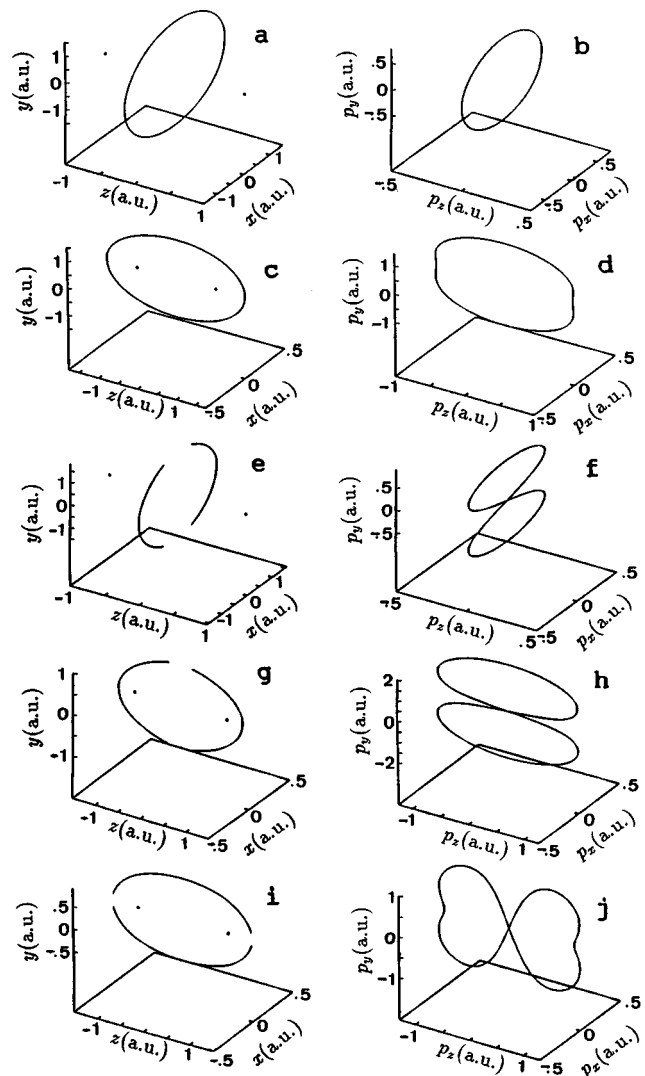


FIG. 2. The orbits of the 3D hydrogen molecule with  $E = -1.0$  and  $R=2.0$ . The dots represent the nuclei. The  $B_{H_2}a$  orbit is shown in (a) and (b),  $B_{H_2}b$  in (c) and (d),  $L_{H_2}a$  in (e) and (f),  $L_{H_2}b$  in (g) and (h), and  $L_{H_2}b'$  in (i) and (j). (a), (c), (e), (g), and (i) represent the Cartesian space coordinates, and (b), (d), (f), (h), and (j) refer to the Cartesian momentum coordinates.

make the first quantization of the H<sub>2</sub> molecule. Bohr's other orbit is the  $B_{H_2}b$ . It is the planetary movement defined by Pauli [3]. This orbit is not an exact ellipse, like the one presented in Fig. 2(c). In the Cartesian momentum coordinates [Fig. 2(d)], it is possible to see the inflections caused by interelectronic repulsion in maximum approximation.

More complicated features can be found in Langmuir orbits ( $L_{H_2}a$ ,  $L_{H_2}b$ , and  $L_{H_2}b'$ ). The  $L_{H_2}a$  orbit is shown in Figs. 2(e) and 2(f) for 3D Cartesian coordinate space and momentum, respectively. In this orbit the angular momentum is extremely variable. The "collision" of electrons is shown in Fig. 2(e). This "collision" appears in Fig. 2(f) as a cross in (0,0) momentum coordinates. Similarly, the  $L_{H_2}b$  and  $L_{H_2}b'$  orbits have the same behavior. The Cartesian space and momentum coordinates for the  $L_{H_2}b$  orbit are shown in Figs. 2(g) and 2(h), respectively. The  $L_{H_2}b'$  orbit is shown in Fig. 2(i). Similar features of the interelectronic repulsion of

the  $B_{H_2}b$  orbit in momentum coordinates can be seen in the  $L_{H_2}b'$  orbit presented in Fig. 2(j). Figures 2(a)–2(j) were made using the complete Hamiltonian [Eq. (3)] with  $E_{el} = -1.0$  and  $R=2.0$ , where  $E_{el}$  is the electronic energy.

The stabilities of the symmetric orbits were studied with the effective Hamiltonian with three degrees of freedom. More details about stabilities (stability angle and Lyapunov exponent) of these orbits can be found in Ref. [6].

The effective Hamiltonian of the three degrees of freedom for neighborhood trajectories for  $B_{H_2}a$  and  $B_{H_2}b$  orbits in confocal elliptic coordinates is given by

$$H_{el} = \frac{4}{R^2(\xi^2 - \eta^2)} \left\{ (\xi^2 - 1)P_\xi^2 + (1 - \eta^2)P_\eta^2 + \left( \frac{1}{\xi^2 - 1} + \frac{1}{1 - \eta^2} \right) P_\varphi^2 \right\} - \frac{8}{R} \frac{\xi}{(\xi^2 - \eta^2)} + \frac{1}{R_{12}}, \quad (6)$$

where  $R_{12} = R(\xi^2 + \eta^2 - 1)^{1/2}$ ,  $\xi = \xi_1 = \xi_2$ ,  $\eta = \eta_1 = -\eta_2$ ,  $\varphi_2 - \varphi_1 = \pi$ ,  $P_\xi = P_{\xi_1} = P_{\xi_2}$ ,  $P_\eta = P_{\eta_1} = -P_{\eta_2}$ , and  $P_\varphi = P_{\varphi_1} = P_{\varphi_2}$ . The symmetric neighborhood of these symmetric orbits is defined by the signals which appear in variables.

The effective Hamiltonian for Langmuir orbits and their neighborhoods are similar to the Eq. (6). For the  $L_{H_2}a$  orbit,  $R_{12} = R[(\xi^2 - 1)(1 - \eta^2)\sin^2(\varphi)]^{1/2}$ ,  $\xi_1 = \xi_2$ ,  $\eta_1 = \eta_2$ ,  $\varphi_2 - \varphi_1 = 2\varphi$ ,  $P_{\xi_1} = P_{\xi_2}$ ,  $P_{\eta_1} = P_{\eta_2}$  and  $P_{\varphi_1} = -P_{\varphi_2}$ . For the  $L_{H_2}b$  orbit,  $R_{12} = R\xi|\eta|$ ,  $\xi_1 = \xi_2$ ,  $\eta_1 = -\eta_2$ ,  $\varphi_2 - \varphi_1 = 0$ ,  $P_{\xi_1} = P_{\xi_2}$ ,  $P_{\eta_1} = -P_{\eta_2}$  and  $P_{\varphi_1} = P_{\varphi_2}$ . Finally, for the  $L_{H_2}b'$  orbit,  $R_{12} = R[(\xi^2 - 1)(1 - \eta^2)]^{1/2}$ ,  $\xi_1 = \xi_2$ ,  $\eta_1 = \eta_2$ ,  $\varphi_2 - \varphi_1 = \pi$ ,  $P_{\xi_1} = P_{\xi_2}$ ,  $P_{\eta_1} = P_{\eta_2}$  and  $P_{\varphi_1} = P_{\varphi_2}$ .

The  $B_{H_2}b$ ,  $L_{H_2}b$ , and  $L_{H_2}b'$  orbits are marginally stable in the azimuthal direction [6], considering only symmetric displacement. For  $\Delta\varphi = \varphi_2 - \varphi_1 \neq 0$  (or  $\pi$ ) the system lost this stability. Other important asymmetries can also be included in the  $H_2$  studies, e.g., to consider  $\xi_1 \neq \xi_2$ ,  $|\eta_1| \neq |\eta_2|$ , etc.

The symmetric orbit can change its stability (stable  $\rightleftharpoons$  unstable) when the trajectory crosses a hyperbolic point in the phase space. The hyperbolic point in the space coordinate for the  $B_{H_2}a$  orbit is shown in Fig. 3 including the centrifugal term. In this case, the trajectories escape from the  $z$  direction, i.e., perpendicular to the orbital plane (unstable direction). The other direction is stable.

This hyperbolic point was found with the Hamiltonian with three degrees of freedom [Eq. (6)], as were the stability angles and Lyapunov exponents. There are three hyperbolic points for the  $L_{H_2}a$  orbit. The presence of these points modifies qualitatively the dynamics of the system. For example, in an axial  $H_2$  system (one dimensional) these points are related to ionic resonance.

### B. Neighborhood of some symmetric orbits

Some neighboring trajectories of the orbits that appear in Fig. 1 have been calculated with the complete Eq. (3). ‘‘Flat ring’’ trajectories can be obtained if the electrons are not limited to the orbital plane of the  $B_{H_2}a$  orbit, considering particular initial conditions. These electrons run approxi-

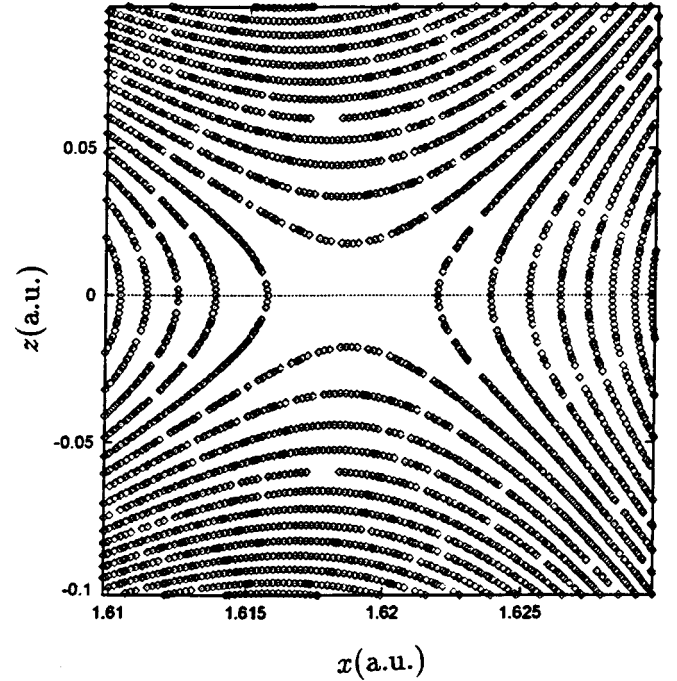


FIG. 3. The level curves of the hyperbolic point in space coordinates for the  $B_{H_2}a$  orbit with  $R=2.0$ . The ordinate belongs to the internuclear axis (unstable displacement) and the abscissa belongs to the orbital plane (stable displacement). Each level corresponds to 5% of  $\Delta E$ .

mately over a section of an ellipsoid (‘‘flat ring’’). In this case, the Poincaré map is ‘‘fuzzy’’ only for a torus far from the orbit.

‘‘Washer’’ trajectories are obtained if the electrons are limited to the orbital plane of the  $B_{H_2}a$  orbit, but not restricted to a circumference (transversal section of the ellipsoid). The Poincaré map is similar to the integrable system, since the other degree of freedom ( $\eta$ ) is not visited with this particular initial condition. This Poincaré map is presented in Fig. 4. Similar maps are obtained for unstable region ( $E_{el} < -1.16$ ).

The combination of the ‘‘flat ring’’ and ‘‘washer’’ trajectories gives the ‘‘ring’’ trajectories, and the related Poincaré map is completely ‘‘fuzzy.’’ The ‘‘ring’’ trajectories far from the  $B_{H_2}a$  orbit suffer autoionization (open torus). The  $L_{H_2}a$  orbit presents ‘‘flat ring’’ and ‘‘washer’’ trajectories, similarly to the  $B_{H_2}a$  orbit.

### C. Unrestricted four-body

When the  $B_{H_2}a$  and  $L_{H_2}a$  orbits are stable for symmetric displacement, the correlated unrestricted four-body problem [Eq. (1)] can also be stable. The neighborhoods of the  $B_{H_2}a$  and  $L_{H_2}a$  orbits without fixed nuclei are presented in Figs. 5(a) and 5(b). These trajectories correspond to  $E_{tot} = -0.5$  and initial  $E_{el} = -1$ . The neighborhood of these orbits is similar to the restricted four-body problem discussed before. The nuclei oscillate like the shape of the sine function, while the electrons orbit around the internuclear axis. The period of the electronic orbit is about 600 times smaller than that of the

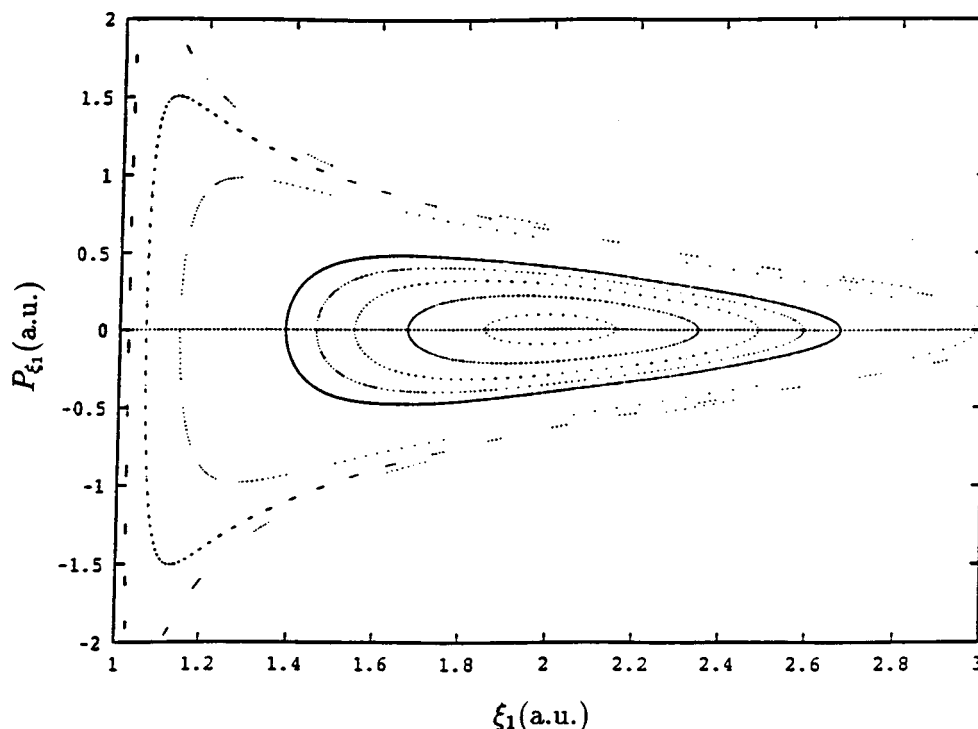


FIG. 4. Poincaré map ( $\varphi_2=0$ ) around the  $B_{H_2}a$  orbit. The initial conditions of symmetric trajectories are:  $\xi_1 = \xi_2 = 2.0$ ,  $\eta_1 = \eta_2 = 0.0$ ,  $\varphi_2 - \varphi_1 = \pi$ ,  $P_{\xi_1} = P_{\xi_2} = P_{\eta_1} = P_{\eta_2} = 0.0$ ,  $-1.0 \leq P_{\varphi_1} = P_{\varphi_2} \leq 1.0$ ,  $R = 2^3/(3^2 - 3^{1/2})$ , and  $E = -(3^{3/2} - 1)^2/2^4$  (the values of  $R$  and  $E$  are given by the Bohr quantization results of the  $B_{H_2}a$  orbit).

nucleus. These studies can also add some knowledge to the stability work of the hydrogenlike molecule [17].

#### D. Pauli's orbits

Some orbits connected to Pauli's work for  $H_2^+$  [3] are discussed.

(a) Satellite trajectory—the electron moves around one proton, and the trajectories are limited between an ellipse and a hyperbola;

(b) Planet trajectory—the electron moves simultaneously around two protons, and these trajectories are limited between two ellipses;

(c) Lemniscat trajectory—similar to the previous case. The difference is that the trajectories are not limited between two ellipses, but describe lemniscat trajectories with shape of “∞”.

The electronic movements in the  $H_2$  system are a combination of two trajectories above, since in this case two electrons are presented. The combinations of the different trajectories renders the system unstable due to autoionization caused by the interaction of the electrons. The  $B_{H_2}b$ ,  $L_{H_2}b$ , and  $L_{H_2}b'$  orbits can be seen as a combination of two planetary symmetric movements; in this particular case, the electrons are strongly correlated.

#### E. One-dimensional trajectories

Trajectories in one dimension can also be found.

(a) Pendulum trajectories (for  $H_2^+$  [3])—the two electrons oscillate along the middle axis (perpendicular to the internuclear axis) between the two protons. The oscillation may be symmetric or asymmetric (chaotic). In the latter case, the

electronic coordinates differ in signals and module. The fundamental orbit for asymmetric pendulum is presented in Fig. 6. There are no pendulum trajectories in atomic systems (Wannier orbit) since they are spherically symmetric.

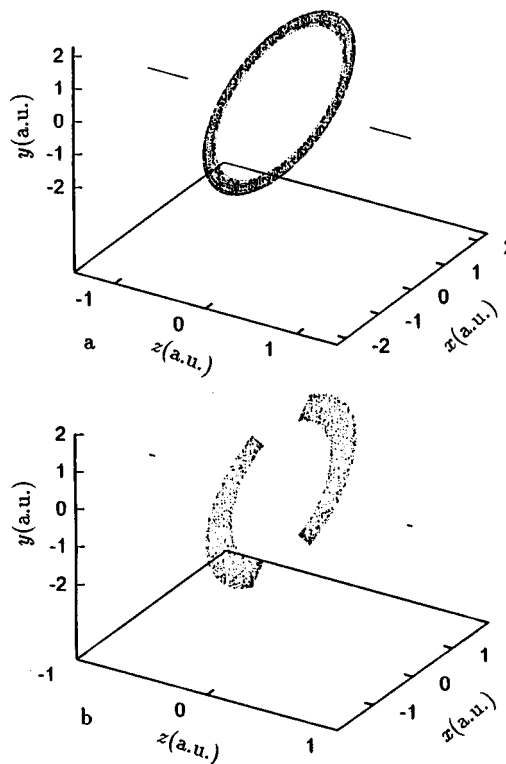


FIG. 5. The neighborhood of the unrestricted four-body  $B_{H_2}a$  orbit in (a) and  $L_{H_2}a$  in (b).

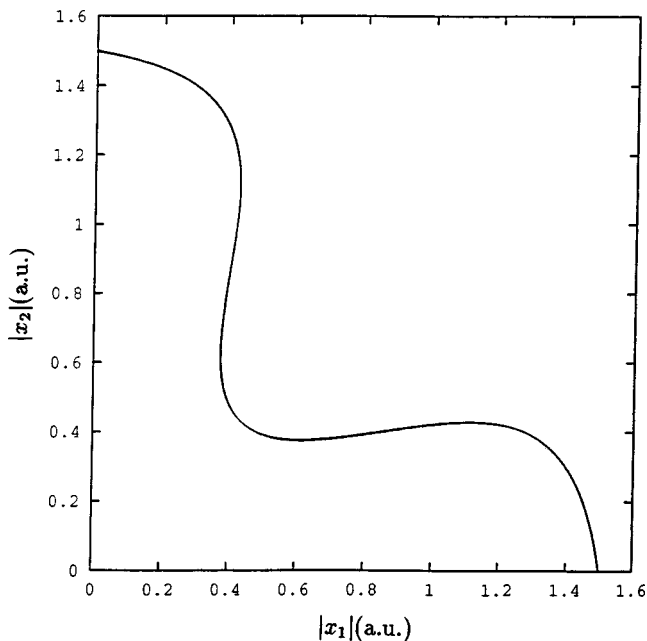


FIG. 6. Fundamental asymmetric pendulum orbit for initial conditions  $x_1 = z_1 = 0$ ,  $x_2 = 1.5$ , and  $z_2 = 0$ ; all momentum are zero, and  $E_{\text{el}} = -2.44$  and  $R = 2.0$ .

The effective Hamiltonian for the symmetric pendulum is given by Eq. (6) with  $R_{12} = R(\xi^2 - 1)^{1/2}$ ,  $\xi_1 = \xi_2$ ,  $\eta_1 = \eta_2 = 0$ ,  $\varphi_2 - \varphi_1 = \pi$ ,  $P_{\xi_1} = P_{\xi_2}$ ,  $P_{\eta_1} = P_{\eta_2} = 0$ , and  $P_{\varphi_1} = P_{\varphi_2}$ .

(b) Axial trajectories—the electrons are in the internuclear axis. Four distinct combinations are possible because there are two electrons and two protons, which divide the internuclear axis into three regions.

These four distinct combinations can be named *eZZe*, *ZeeZ*, *ZeZe*, and *ZZee* considering the two nuclei (*Z*) and the two electrons (*e*). The *eZZe* configuration has the electrons in two outer regions of the molecule, and the *ZeeZ* configuration has the electrons inside the molecule. The *ZeZe* (or *eZeZ*) configuration has one electron inside and another outside the molecule. The *ZZee* (or *eeZZ*) configuration has the two electrons in the same outer region of the molecule. This last configuration is very similar to the “frozen planetary atom” (FPA) of the helium atom [9,10].

In the case of  $\text{H}_2$  in one dimension a FPA configuration can be found. The Poincaré map of this FPA configuration shows tori, which represents the intermediate case between He and the negative hydrogen ion ( $\text{H}^-$ ). Calculations of stability indexes for the  $\text{H}_2$  system in four degrees of freedom (with  $R = 2$ ) show unstable behavior of the FPA orbit. These previous calculations give  $\lambda_r = 0.3$  and  $\lambda_\theta = 0.4$  for  $E_{\text{el}} = -1.0$ , where  $\lambda_r$  and  $\lambda_\theta$  are the Lyapunov exponents for radial and angular motion, respectively. The FPA configuration for the  $\text{H}_2$  system in two dimensions is unstable since the inner electron blinds the nearby proton totally, and the outer electron is attracted by the other proton on the opposite side of the molecule. The configuration assumed by the molecule is the inner electron orbiting in a satellite trajectory around one proton and the outer electron orbiting in a planet trajectory around the set consisting of the other proton and the satellite system. This configuration, as well as one with each electron orbiting in different planet trajectories around

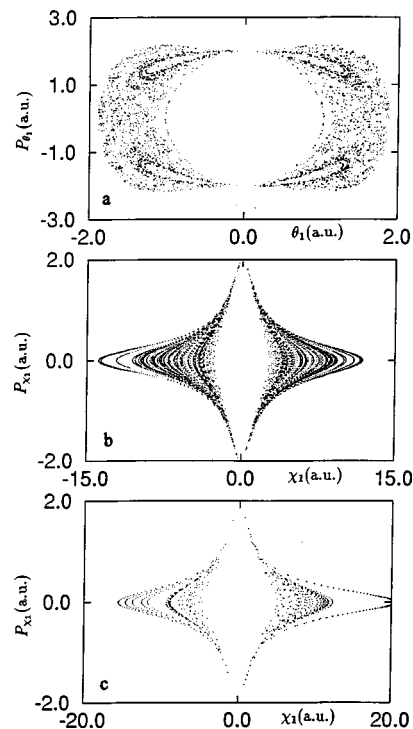


FIG. 7. Poincaré maps ( $z_2 = -R/2$ ) with  $R = 2.0$  for (a) *ZeeZ* configuration with initial conditions  $z_1 = -z_2 = 0.5$  and  $P_{z_1} = P_{z_2} = 1.82574$  ( $E_{\text{el}} = -1.00$ ); (b) *ZeZe* configuration with initial conditions  $z_1 = 5.0$ ,  $z_2 = -0.5$ , and  $P_{z_1} = P_{z_2} = 0.0$  ( $E_{\text{el}} = -2.90$ ); (c) *eZZe* configuration with initial conditions  $z_1 = 5.0$ ,  $z_2 = -2.5$ , and  $P_{z_1} = P_{z_2} = 0.0$  ( $E_{\text{el}} = -1.24$ ).

the two protons, can be studied using a dipole approximation, like the FPA for He atom [18]. The three other combinations in one dimension (axial) show chaotic behavior for asymmetric trajectories. These configurations are similar to the *eZe* configuration of He [9]. Some Poincaré maps with one electron over one nucleus ( $z_2 = -R/2$ ) were calculated for these three axial configurations. Figure 7(a) shows the map for *eZZe* configuration, Fig. 7(b) shows the *ZeZe* configuration, and Fig. 7(c) shows the *ZeeZ* configuration. The regularized coordinates are shown in these figures, as long as the Cartesian momentum coordinates diverge over the proton.

The near-collinear intrashell resonances for He system are associated with an asymmetric stretchlike motion of the electron pair. The axial and pendulum configurations are probably important to describe the similar resonances in the  $\text{H}_2$  system. The *eZZe* configuration is very similar to that of *eZe* for He [9]. This configuration can be important to describe the Rydberg molecular state with atomic character. On the other hand, the *ZeeZ* configuration can describe states with molecular character, since interaction between the electrons is strong (the electron-exchange process). The *ZeZe* configuration can be considered an intermediate case, and the pendulum configuration can be similar to that of *ZeeZ*. The use of asymmetric orbits in one dimension, similarly to the He atom [19], can be considered in the study of  $\text{H}_2$  system, but here only symmetric orbits have been used.

## F. Regularized and smoothed potential

Important points may be discussed in relation to the regularized and smoothed potentials [Eq. (5)] for 1D system with

two or more electrons. The procedure of regularization modifies the 1D Hamiltonian. The modification is the addition of a centrifugal barrier in the singularities. For example, the canonical transformation ( $Q^2=x$ ) of the regularization of the hydrogen atom (in one dimension) changes the electronic coordinate ( $x$ ) by the harmonic-oscillator coordinate ( $Q$ ) becoming  $x \geq 0$ . This modification restricts the electron to occupying only the positive “side” of the H in one dimension. This is interpreted as addition of the centrifugal barrier for parabolic trajectories in one dimension with  $e=1$ .

This modification does not change the physics of the H atom, since H has a symmetric plane containing the barrier, and the variable  $x$  appears as  $|x|$  in the correct 1D Hamiltonian of the H atom. Whether or not the barrier is added changes the He atom (two-electron system) completely [9,10].

The procedure of regularization does not change the Hamiltonian for the  $H_2^+$  (one-electron) system; it just keeps the outer and inner regions separated, since the potentials are singular. Similarly, the physical modifications of the He atom are also observed in the  $H_2$  system in one dimension.

The presence or absence of the centrifugal barrier is important in 1D movements. The  $Zee$  and  $eZe$  configurations are different in the He atom, since the  $Zee$  configuration is classically stable whereas the  $eZe$  configuration is unstable [9]. The (smoothed) potential without centrifugal barrier cannot be similar to the potential with barrier [10], because the latter links the  $Zee$  and  $eZe$  configurations.

The 1D potential with barrier is used for high-eccentricity orbits in the free atom and for the FPA in the radial variable, since the relative angle is zero most of the time [10]. The 1D smoothed potential (without barrier) is used when the nucleus exercises just a perturbation in the electronic movements [20].

The electrons collide with each other and with the nuclei in 1D movements. These collisions rarely occur for higher dimensions. However, the use of the smoothed potential reduces the importance of the collisions, while the smoothed parameter is an important adjustment factor.

Briefly, the difference between these potentials occurs for the two-plus electron system in one dimension. The potentials are equivalent for a one-electron system (one or two dimensions) and a two-plus electron system in two dimensions, with the exception of the “role of the Coulomb singularity” [21]. The stability of the axial  $H_2$  system with a smoothed potential without barrier depends on the  $\delta$  parameter [see Eq. (5)] and on the four axial configurations, since this smoothed potential connects these axial trajectories with different stabilities. The level curves of the smoothed potential energy is presented in Fig. 8 with  $R=2.0$  and  $\delta=1.0$  for the  $H_2$  system in one dimension. Each level curve corresponds to 5% of the  $\Delta E (=E_{\text{minimum}} - E_{\text{maximum}})$ , and the coordinates refer to the position of the electrons. The choice of  $\delta=1.0$  (one atomic unit) is related to the quantum average minimum distance in atomic or molecular systems [20]. This implies that the classical model does not have singular potential, like quantum mechanics does.

The connections of the axial trajectories by a smoothed potential can be seen in Fig. 8. The  $ZZee$  (or  $eeZZ$ ) and  $eZZe$  quadrants (Fig. 8) appear in the He atom as  $Zee$  and  $eZe$  configurations [9], respectively, for smoothed and sin-

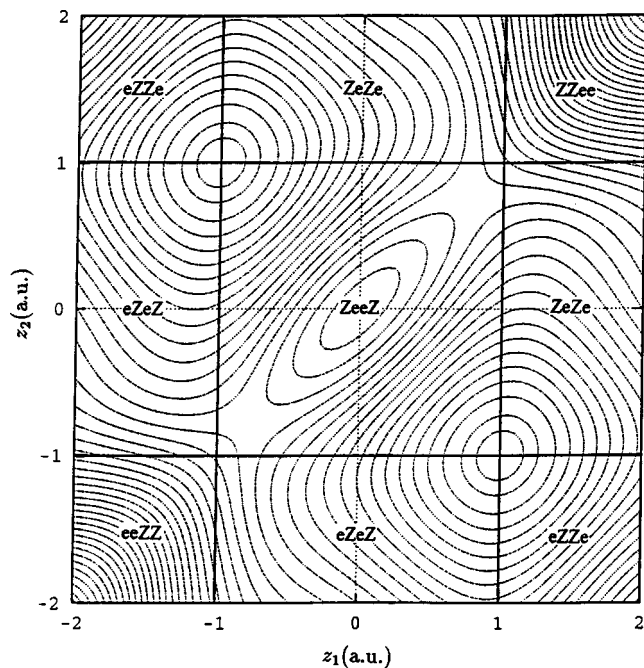


FIG. 8. Smoothed potential energy for the  $H_2$  system in one dimension. Each level corresponds to 2.5% of  $\Delta E$ ,  $R=2.0$ , and  $\delta=1.0$ .

gular potentials. The  $H_2$  and He potentials coincide in the  $R \rightarrow 0$  limit.

The other configurations ( $ZeZe$  or  $eZeZ$  and  $ZeeZ$ ) are exclusive of the  $H_2$  system. The  $ZeeZ$  configuration shows a maximum in (0,0) coordinates that represents the electron-electron smoothed collision. This collision ( $z_1=z_2$  diagonal) presents two minimums (hyperbolic point) near protons [triple collisions or ionic resonance ( $H^-H^+$ )]. This triple collision was shifted in the  $ZeeZ$  direction because of the smoothed procedure. For the exact potential (singular) this collision appears in  $(-1,-1)$  and  $(1,1)$  coordinates. The two simultaneous electron-proton collisions [covalent resonance ( $H-H$ )] appears in  $ZeeZ$ ,  $ZeZe$  or  $eZeZ$ , and  $eZZe$  as absolute minimums.  $ZeZe$  or  $eZeZ$  and  $eZZe$  configurations present similar features to  $ZeeZ$  except for the electron-electron collision. The  $ZeeZ$  configurations can be autoionized with a smoothed potential, but this is impossible with regularized potential.

Briefly, what is the best potential (regularized and smoothed) model that represents the two-(more-) electron system in one dimension? Actually the physical system is 3D. The system can be reduced to 2D if the angular momentum is preserved. The subsequent reduction of the dimension depends on the studied trajectories of the system. It is necessary to maintain the centrifugal barrier in one dimension for higher eccentricity and for some correlated trajectories. The centrifugal barrier potential appears explicitly in the Hamiltonian in curvilinear coordinates. This is reduced in one dimension considering an infinity barrier on the nuclei. This barrier impedes the electron from “falling” into the nucleus. The addition of this barrier can be made using the regularization procedure or, *ad hoc*, in the smoothed potential. The smoothed potential (without barrier) can be recommended for a nonisolated system when the nuclei are considered a perturbation, e.g., in atoms and molecules in a strong

electric field [20]. If the interest of the study is to describe generic 2D trajectories and not to represent high eccentricity ones, the 1D smoothed potential without barrier is indicated. The smoothed parameter ( $\delta$ ) can be considered the other dimension, approximately. The electron-nucleus and electron-electron collisions are drastically reduced, as in two dimensions.

### G. Semiclassical quantization

The actions of the symmetric orbits can be calculated as

$$S^{\text{Bohr}} = 2\pi(n+0)$$

for Bohr orbits (rotation), and as

$$S^{\text{Langmuir}} = 2\pi(n+1/2)$$

for Langmuir orbits (libration). Nevertheless, the system in three dimensions has other degrees of freedom, and these are added in the actions as

$$S^{\text{Bohr}} = 2\pi[n+0 + \theta_o(l+1/2) + \theta_p(m+1/2)]$$

and

$$S^{\text{Langmuir}} = 2\pi[n+1/2 + \theta_o(l+1/2) + \theta_p(m+1/2)],$$

where  $\theta_o$  and  $\theta_p$  are the stability angles for symmetric displacements (librations) which belong to the orbital plane and to the perpendicular orbital plane, respectively.

The vertical spectrum for one orbit, i.e., the eigenvalues for fixed geometry ( $R$ ) can be obtained by the following procedure: the action [ $S(n,l,m)(E)$ ] as a function of the quantum numbers ( $n$ ,  $l$ , and  $m$ ) and of the energy ( $E$ ) is calculated, while the intersection between the values of the energy for  $S(n,l,m)(E)$  and for classical calculation of the action [ $S^{\text{classical}}(E)$ ] (with  $R$  fixed) is considered the eigenvalue ( $E_n$ ) of the orbit. Since the  $H_2$  system is not scaled to energy, the relationship between  $E$  and  $S$  is calculated numerically. The eigenvalues for other geometries can be found using the  $R$  scaling relation given by

$$S = \tilde{S}(R/2)^{1/2}$$

and

$$E = \tilde{E}(2/R).$$

The function  $\tilde{S}(n,l,m)(\tilde{E})|_{R=2}$  and  $\tilde{S}^{\text{classical}}(\tilde{E})|_{R=2}$  can be calculated for several values of  $R$  with scaling relation.  $S(n,l,m)(E)$  depends on scaling in the  $\theta(E)$ , since the  $E$  changes with  $R$  and  $\theta$  does not depend on  $R$  parameter,  $\theta$  are the stability angles.  $S^{\text{classical}}(E)$  depends completely on the scaling relation. The eigenvalues can be found making the interception of the  $S(n,l,m)(E)|_R$  and  $S^{\text{classical}}(E)|_R$  curves for each  $R$ .

These eigenvalues for  $B_{H_2}a$  and  $L_{H_2}a$  orbits are shown in Fig. 9 for five first values of  $n$  ( $l=0$  and  $m=0$ ) and several values of  $R$ . The total energy in function of  $R$  for  $B_{H_2}a$  orbit with  $\theta(E)=0$  is shown in Fig. 9(a). The lowest state ( $n=1$ ) presents the minimum ( $E_{\min}=-1.1005$ ) at  $R_{\min}=1.101$ . This value is the same as Bohr's result for  $B_{H_2}a$  orbit quantization [ $E_{\min}=-\frac{1}{2}(3^{3/2}-1)^2/(2^4n^2)$  and  $R_{\min}=\frac{2^3n^2}{3^2-3^{1/2}}$ ] [1]. The other states ( $n$ ) obey the same relations.

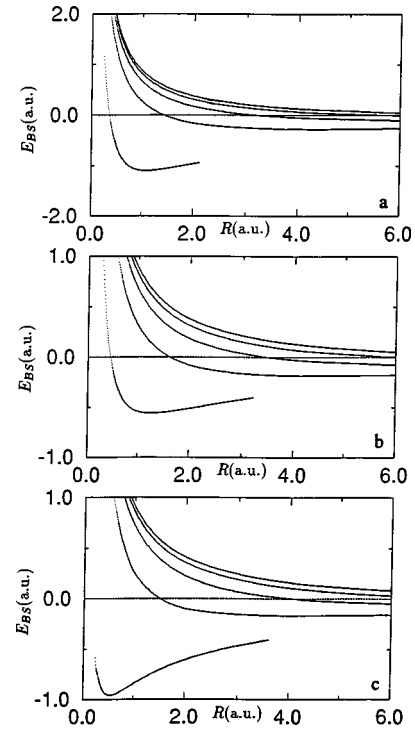


FIG. 9. Bohr-Sommerfeld total energy for several states in function of the  $R$  for (a) the  $B_{H_2}a$  orbit with  $\theta(E)=0$ , (b) the  $B_{H_2}a$  orbit with correct  $\theta(E)$ ; (c) the  $L_{H_2}a$  orbit with correct  $\theta(E)$ .

The eigenvalues for  $B_{H_2}a$  and  $L_{H_2}a$  orbits with correct  $\theta(E)(\neq 0)$  are shown in Figs. 9(b) and 9(c), respectively.  $E_{\min}=-0.5606$  ( $n=1$ ) for the  $B_{H_2}a$  orbit with  $R_{\min}=1.270$  and  $E_{\min}=-0.9552$  ( $n=0$ ) for  $L_{H_2}a$  with  $R_{\min}=0.54$ . This semiclassical quantization occurs in the stable region for the  $B_{H_2}a$  orbit [Fig. 9(b)], i.e.,  $\theta(E)\neq 0$  and  $\lambda=0$ , and  $\lambda$  is the Lyapunov exponent. The first states for the  $L_{H_2}a$  orbit [Fig. 9(c)] belong to the stable region. The other states occur in an unstable region, but this is no longer important since the function  $S(n,l,m)(E)$  practically depends on  $n$  (for a high value of  $n$ ). Those results do not satisfactorily describe the ground state of the  $H_2$  molecule, as expected. The WKB quantization of  $B_{H_2}b$ ,  $L_{H_2}b$ , and  $L_{H_2}b'$  orbits are performed in a similar way. The ground state related to these orbits is very low in energy, making it difficult to obtain the classical action numerically. For excited states, Bohr's orbits present similar eigenvalues and so do Langmuir's.

The rigorous EBK (Einstein-Brillouin-Keller) quantization of invariant KAM tori around Bohr's and Langmuir's orbits is not applicable to the  $H_2$  system, since asymmetric librations are unstable. However, the semiclassical path-integral quantization of nonintegrable Hamiltonian systems [22] is applicable. A better semiclassical description can be obtained using the Gutzwiller trace formula [22] to calculate the density of levels.

### H. Semiclassical path-integral quantization of nonintegrable Hamiltonian systems

The extension of the quantization for most nonintegrable systems is unknown. However, global quantization using the classical periodic orbits is an alternative.

The quantization for a nonintegrable system was made by Gutzwiller using the Feymann path integral in the semiclassical approximation (stationary phase) [22]. The semiclassical density of states (trace formula) depends on classical trajectories which start and end at the same point. These trajectories are the periodic orbits, and they give an oscillatory contribution in the density of states as

$$d(E) = \sum_r \frac{T_r}{\pi\hbar} \sum_{j \neq 0} \frac{\cos[j(S_r/\hbar - \alpha_r \pi/2)]}{|[\det(\mathbf{M}_r^j - \mathbf{1})]^{1/2}|}. \quad (7)$$

The trace formula above sums all repetitions ( $j$ ) of the primitive periodic orbits ( $r$ ) with period  $T_r$ , action  $S_r$  and Maslov index  $\alpha_r$  ( $\alpha_r=0$  for Bohr orbits and  $\alpha_r=2$  for Langmuir orbits),  $\mathbf{M}_r$  is the stability matrix. The determinant of the trace formula depends on the fixed point. In two degrees of freedom, it is given as

$$\left(\frac{1}{2}\right)[\det(\mathbf{M}_r^j - \mathbf{1})]^{1/2} = \begin{cases} -i \sinh(j\lambda/2); & \text{hyperbolic} \\ \cosh(j\lambda/2), & \text{inverse hyperbolic} \\ \sin(j\pi\theta), & \text{elliptic,} \end{cases}$$

where  $\lambda$  is the Lyapunov exponent and  $\theta$  is the stability angle. For  $B_{H_2}b$ ,  $L_{H_2}b$ , and  $L_{H_2}b'$  orbits, only elliptic solutions are found. The singular spectrum is obtained with all repetitions of the primitive orbits in the Gutzwiller formula. The spectrum is smoothed for a finite number of the repetitions, e.g., fixing a maximum period ( $T_{\max}$ ).  $T_{\max}$  was considered as the period of the  $B_{H_2}a$  orbit ( $T_{B_{H_2}a}$ ), since this period is longer than the others considered here. For the  $L_{H_2}a$  orbit it is not necessary to make repetitions, because its period ( $T_{L_{H_2}a}$ ) and  $T_{B_{H_2}a}$  are near. The other orbits are summed once or twice depending on the ratio  $T_i/T_{B_{H_2}a}$ , where  $T_i$  is the period of the orbit considered. The ratio  $T_i/T_{B_{H_2}a}$  changes according to energy, since the system is not scaled to energy. The number of the repetitions is  $\text{Int}[T_i/T_{B_{H_2}a}]$ , where  $\text{Int}[X]$  is the entire part of the  $X$ .

The  $B_{H_2}b$ ,  $L_{H_2}b$ , and  $L_{H_2}b'$  orbits are reduced to two degrees of freedom, since the azimuth direction degree is marginally stable for these symmetric orbits [6]. The eigenvalues of the monodromy matrix are not complex numbers (loxodromic), i.e., they are imaginary (elliptic) or real (hyperbolic). These eigenvalues are real numbers for the three degrees of freedom  $B_{H_2}a$  and  $L_{H_2}a$  orbits [6]. Since these two orbits have two uncoupled (two linearly independent or nonloxodromic eigenvalues pairs) degrees of freedom (small displacements belong to the orbital plane and the perpendicular-to-orbital plane), every three-degree-of-freedom orbit can be broken in two different orbits with two degrees. For instance, the  $B_{H_2}a$  and  $B_{H_2}b$  orbits can be seen as sections of the respective ellipsoid in three dimensions. The three orbits of the two degrees of freedom obtained from  $B_{H_2}a$  (two orbits) and  $B_{H_2}b$  (one orbit) describe a symmetric displacement of the ellipsoid in three dimensions. In addition, see the Poincarè map (Fig. 4) and the discussions in the ‘‘neighborhood of some symmetric orbits’’ about the behavior around the  $B_{H_2}a$  and  $L_{H_2}a$  orbits.

The Gutzwiller formula can be calculated using these seven orbits with two degrees of freedom: two for each  $B_{H_2}a$  and  $L_{H_2}a$  orbit and one for each  $B_{H_2}b$ ,  $L_{H_2}b$ , and  $L_{H_2}b'$  orbit. The related semiclassical density of states in two degrees of freedom for  $R=2$  is presented in Fig. 10(a). The trace formula was extended in order to use orbits with three degrees of freedom, where some orbits ( $B_{H_2}b$ ,  $L_{H_2}b$ , and  $L_{H_2}b'$ ) have one additional constant of the motion (angular momentum in azimuth direction). A similar spectrum for the two degrees of freedom is obtained considering  $m=0$  ( $m$  is the azimuth quantum number), as shown in Fig. 10(b). In the abscissa of Fig. 10 one will find  $(-E_{\text{el}})^{-1/2}$  or the effective quantum number ( $N_{\text{eff}}$ ), while the ordinate shows the density of states [ $d(E_{\text{el}})$ ] divided by square of the  $T_{B_{H_2}a}[d(E_{\text{el}})/T_{B_{H_2}a}^2(E_{\text{el}})]$ . The vertical lines in these figures are the quantum eigenvalues (discussed below). Some singularities appear in these figures; they are related to the change of stability. These changes occur when  $\lambda$  and  $\theta$  are zero or 1 and the denominator of the trace formula becomes null.

The singularities in  $E_{\text{el}} = -1.23$  ( $N_{\text{eff}}=0.90$ ),  $E_{\text{el}} = -0.60$  ( $N_{\text{eff}}=1.3$ ), and  $E_{\text{el}} = -0.36$  ( $N_{\text{eff}}=1.7$ ) concerns the  $L_{H_2}a$  orbit. The singularity in  $E_{\text{el}} = -1.16$  ( $N_{\text{eff}}=0.93$ ) belong to the  $B_{H_2}a$  orbit. The last singularity [ $E_{\text{el}} = -0.95$  ( $N_{\text{eff}}=1.02$ )] appears due to the repetition of the  $L_{H_2}b$  orbit. The dotted curves presented in Fig. 10 are the non-normalized smoothed quantum spectrum divided by  $T_{B_{H_2}a}^2$ . The smoothed quantum spectrum is given by

$$d_Q(E) = (\Delta E \sqrt{2\pi})^{-1} \sum_n e^{-(E-E_n)^2/(2\Delta E^2)},$$

where  $E_n$  are the quantum eigenvalues and  $\Delta E = \hbar/T_{B_{H_2}a}$ .

The spectra calculated by Gutzwiller formula, presented in Fig. 10, are very smooth since they did not include many repetitions. The trace formula sums all primitive orbits [Eq. (7)], but in this calculation only the Bohr and Langmuir orbits were included. These orbits are considered the most important symmetric ones, but the symmetric pendulum orbit can be important too.

The semiclassical calculations take into account some qualitative aspects of the ground state. These calculations describe the eigenvalues of the first states very well, and of the excited states near  $N_{\text{eff}} \approx 1.8$  satisfactorily. Unfortunately the quantum calculation becomes difficult for high  $N_{\text{eff}}$ , and no more quantum results are shown. However, the semiclassical prevision can be used to describe the  $H_2$  system at high  $N_{\text{eff}}$ .

## I. Quantum calculation

An *ab initio* quantum calculation was made for fixed geometry ( $R=2.0$ ). The states calculated are the doubly occupied symmetric excited states (DOSES). These states are related to classical symmetric orbits, since the two electrons describe similar classical trajectories and, consequently, the quantum numbers are equal, except for spin numbers.

The Schrödinger equation for  $H_2$  molecule was calculated using the MELD program [23]. This program uses as an initial

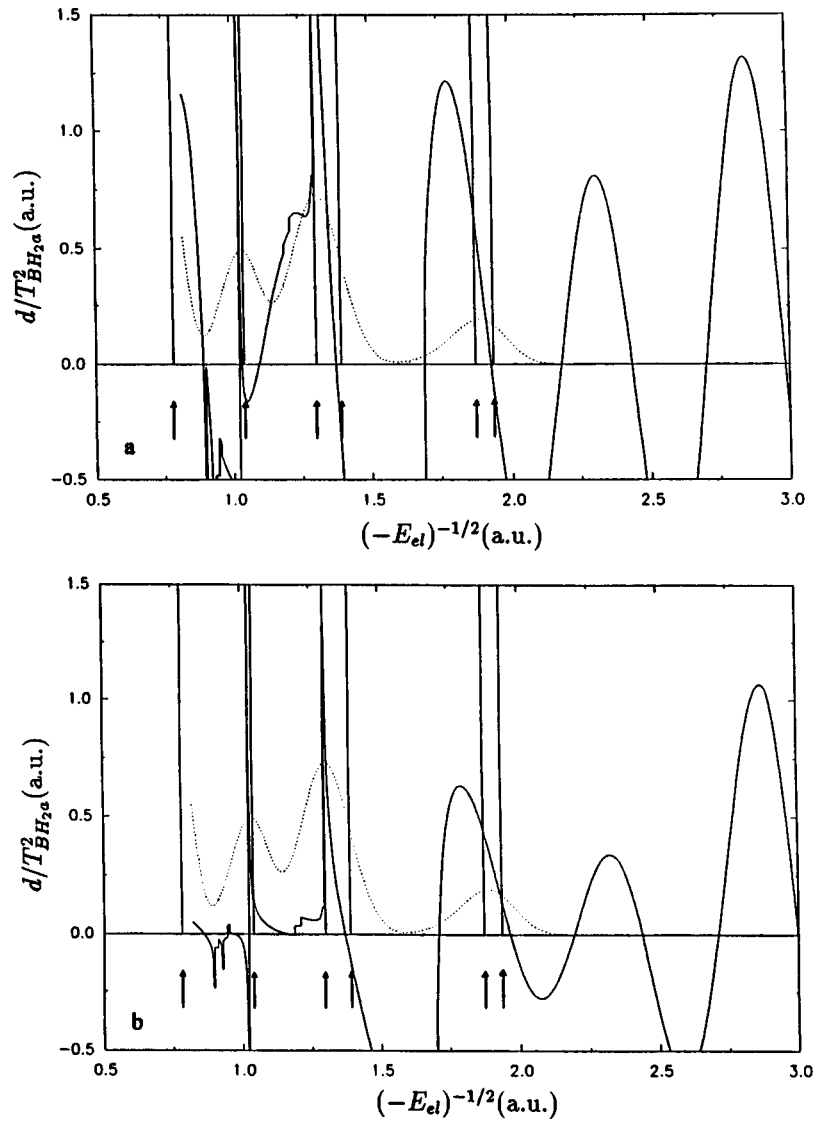


FIG. 10. The  $d$  function is given by Eq. (7) with  $R=2$ . The vertical lines are the quantum eigenvalues. The dotted curves are the smoothed quantum spectrum. (a)  $d$  is calculated in two degrees of freedom. (b)  $d$  is calculated in three degrees.

guess a linear combination of the Cartesian Gaussian atomic bases. These atomic bases comprise  $9s$ ,  $6p$ ,  $4d$ ,  $3f$ , and  $2g$  atomic functions. The electronic structure was described at the full configuration-interaction level, and, having a Hartree-Fock configuration, as the zero-order function.

The DOSES are resonances. This particularity renders the quantum calculation very difficult. The quantum calculation performed here considers the resonance states as discrete ones, which represent an important limitation to the calculation.

The resonance characteristic of DOSES can be seen in Table I. For example,  $1\sigma_u^2$  DOSES has energy above that of the  $1\sigma_g^1$  (ground-state) of the  $H_2^+$  system. The  $H_2^+$  can be considered as a  $H_2$  system with one ionized electron (electron infinity far). All DOSES are inside the ionization series of  $H_2$ . The limit series correspond to the  $H_2^+$  spectrum [5]. The DOSES calculated are singlet and have  $\Sigma_g^+$  symmetry in the  $D_{\infty h}$  group. The symmetry of the  $H_2^+$  doublet states appear between parentheses in Table I. The number of the ionization series (continuum) increases as number of the DOSES. The quantum calculation made here has been im-

portant to give an idea about the DOSES.

The quantum calculation is compared to others in the literature. The total energy ( $E$ ) of the first DOSES was calculated as  $E = -0.3985$  [24],  $E = -0.3969$  [25],  $E = -0.402$

TABLE I. Total energy ( $E = E_{el} + 1/R$ ) in a.u. for the  $H_2$  ground state and DOSES and for  $H_2^+$  [5] with  $R=2.0$ .

State	$E_{H_2\text{-DOSES}}$	$E_{H_2^+}$	
$1\sigma_g^2$	-1.138		
$1\sigma_g^1$		-0.603	( $X \Sigma_g^+$ )
$1\sigma_u^2$	-0.427		
$1\sigma_u^1$		-0.168	( $A \Sigma_u^+$ )
$1\pi_u^2$	-0.0928		
$2\sigma_g^2$	-0.0185		
$1\pi_u^1$		+0.071	( $B \Pi_u^+$ )
$2\sigma_g^1$		+0.139	( $C \Sigma_g^+$ )
$3\sigma_g^2$	+0.215		
$2\sigma_u^2$	+0.233		

[26], and  $E = -0.427$  (this work).  $E = -0.09437$  [25] for the second DOSES can be compared with  $E = -0.0928$  (this work).

The  $(1\sigma_u^1)(2\sigma_u^1)$  state that is not one of the DOSES is used to compare with the results in literature.  $E = -0.234$  is found in this work, while the value  $E = -0.2372$  was found in Ref. [24], and  $E = -0.2369$  was found in Ref. [25].

Several quantum methods can be applied to calculate the  $H_2$  system. The perturbation theory is used for weakly correlated electronic movements. For example, the perturbation theory uses the expansion of the interelectronic distance ( $r_{ij}$ ), e.g., in series of the Legendre polynomials, to describe the He atom [27]. That expansion given Neumann formula [28], together with the zero-order wave function of the  $H_2^+$  molecule ion, can be used to describe the  $H_2$  molecule. This method probably converges slowly to strong correlated movements such as DOSES, and special treatment such as Feshbach projection must be done in order to describe the resonance states.

The quantum solution of the He system has been obtained transforming the Schrödinger equation into perimetrical coordinates [9,29]. However, the loss of spherical symmetry in the  $H_2$  system renders the use of this procedure difficult.

The smoothed semiclassical spectra for the  $H_2$  system presented in Fig. 10 try to predict the DOSES eigenvalues or the smoothed quantum spectrum, although the quantum eigenvalues are not good for higher DOSES. If these semiclassical calculations are good, the quantum eigenvalue for  $2\sigma_g^2$ ,  $3\sigma_g^2$ , and  $2\sigma_u^2$  states would be lower than the ones calculated in this work. For example, the fourth and fifth DOSES appear in  $N_{\text{eff}} \approx 1.9$  for quantum calculations, and in  $N_{\text{eff}} \approx 1.8$  for semiclassical ones. The semiclassical prevision can then be obtained as  $E_{\text{el}} = -0.32$  for the fourth ( $3\sigma_g^2$ ) state and  $E_{\text{el}} = -0.30$  for the fifth ( $2\sigma_u^2$ ) state, if the separation of these states is similar to that in the quantum calculation. Some semiclassical calculations were performed for each orbit in order to correlate the orbit with the DOSES. For the ground state the principal contributions are given by the  $B_{H_2}a$  and  $L_{H_2}a$  orbits. The first of the DOSES is described mainly by the  $L_{H_2}b$  orbit and a few of the rest by  $B_{H_2}b$  and  $L_{H_2}b'$ . For the other DOSES the most important contribution is given by the  $L_{H_2}a$  orbit. Another semiclassical calculation is made with Bohr and Langmuir orbits separately, showing that the Langmuir orbits are the most important to describe these DOSES.

Correlation between the classical orbit and the shape of the probability density of the molecular orbitals can also be made. The trajectories around the  $B_{H_2}a$  and  $B_{H_2}b$  orbits are similar to probability level curves associated with  $\sigma_g$  molecular orbital of the  $H_2$  molecule.  $\pi_u$ , in the same way, can be correlated to  $L_{H_2}a$  and  $L_{H_2}b'$  orbits. For instance, the most important contributions of the orbits in the description of the DOSES are given by the  $L_{H_2}b$  orbit in  $1\sigma_u^2$  state (first of the DOSES) and the  $L_{H_2}a$  orbit in  $1\pi_u^2$  state (second of the DOSES). The shape of the  $L_{H_2}b$  orbit [Figs. 1 and 2(g)] is just like that of the  $1\sigma_u$  molecular orbital, since they have a nodal plane between the protons. Similarly, the  $L_{H_2}a$  orbit [Figs. 1 and 2(e)] has a nodal plane that contains the protons,

like the  $1\pi_u$  molecular orbital. These correlations are not accidental; probably the “scars” around some classical orbit appear in eigenfunctions of some excited state or in the wave function of some set of them.

### J. Experimental measure proposal

The stable  $A_2^{2+}$  molecule-ions (where  $A_2^{2+}$  can be  $Be_2^{2+}$ ,  $Mg_2^{2+}$ ,  $Ca_2^{2+}$ ,  $C_2^{2+}$ ,  $N_2^{2+}$ ,  $O_2^{2+}$ , etc.) can be required for experimental measure of the  $H_2$  DOSES. Since the ground state of these  $A_2^{2+}$  molecule ions is bounded (stable) [30] and all DOSES are not bounded. The  $A_2^{2+}$  molecule ions can contain two more nonbinding electrons in the Rydberg state, which do not interfere with the core. These final  $A_2$  molecules allow for the use of spectroscopy techniques and not just the collision ones for the measures of the resonance DOSES.

## IV. DISCUSSION

Several studies for the  $H_2$  molecule were shown in this paper. These studies are important for a future understanding of the connection between classical and quantum worlds (“the correspondence principle”) to chaotic problems and of the chemical bond since the  $H_2$  system contains the basic ingredients (two-electron binding) for that.

There are several works in literature on the He atom [9,16,19,27,29], but not on the  $H_2$  molecule [6]. An extension was made in the He system in order to obtain the  $H_2$  system, and consequently several calculation techniques used in He studies can be applied in the  $H_2$  system.

The importance of the regularized Hamiltonian and the symmetric classical orbits and their stabilities were described partially in Ref. [6]. More complete discussions were made here. The effective Hamiltonians of the three degrees of freedom to calculate the stability indexes were presented. The neighborhoods of some symmetric orbits were presented, along with some Poincarè maps to show their quasi-integrable behavior. Unrestricted-four-body symmetric trajectories were described, which can be important in stability studies of the hydrogenlike molecule or in generic four-body problems. The possibilities of studies of the  $H_2$  molecule in one dimension for pendulum and axial trajectories were described. The axial  $H_2$  molecule presents a more complex configuration in relation to the He atom. Important calculations using the symbolic dynamics can be made with this model as with the He atom [9]. Discussions on the use of the regularized and smoothed potential were presented. They are important since the 1D models are not generically correct.

Some Bohr-Sommerfeld quantizations were performed for the symmetric orbits, but those calculations were not enough to describe the  $H_2$  system. Unfortunately, that system is not integrable, and can show chaotic behavior and a global semiclassical quantization must be made. The Gutzwiller formula was calculated using the symmetric orbits. That semiclassical approach showed its importance to describe the nonintegrable and multidimensional  $H_2$  molecule with a few orbits. Those symmetric classical orbits describe the DOSES; other classical orbits can describe other states. Several types of orbits can be used, e.g. 1D orbits and asymmetrical ones. Specifically, the correct semiclassical quantization of the DOSES might have been achieved in these

studies, and the quantum calculation was used to show it. In addition, semiclassical calculations predict that the *ab initio* quantum calculation must be improved in order to describe the highly excited DOSES. The improvement of the quantum calculations to describe resonance states has been shown in the literature [24–26], but is not enough for now. The semiclassical approach can also be considered a very important method to substitute for quantum calculations when the latter presents practical problems. The semiclassical prevision can be used to describe the H<sub>2</sub> system at high  $N_{\text{eff}}$ .

Mainly, this paper described a theoretical study of the nonlinear dynamics of the hydrogen molecule. This is a first

step toward understanding the correspondence principle in the chemical world that treats essentially nonlinear systems.

#### ACKNOWLEDGMENTS

The author acknowledges Dr. M. A. M. de Aguiar for useful discussions and Dr. F. Machado and Dr. R. Custódio for providing the MELD codes and the atomic bases, respectively. Financial support from FAPESP (Project Nos. 1995/9563–8 and 1996/9862–7) and partial infrastructure from the Instituto de Física “Gleb Wataghin” (UNICAMP) is also acknowledged.

- 
- [1] N. Bohr, *Philos. Mag.* **25**, 10 (1913); **26**, 476 (1913); **26**, 857 (1913).
- [2] H. Kragh, *J. Chem. Educ.* **54**, 208 (1977).
- [3] W. Pauli, Jr., *Ann. Phys. (Leipzig)* **68**, 177 (1922).
- [4] M. P. Strand and W. P. Reinhardt, *J. Chem. Phys.* **70**, 3812 (1979).
- [5] D. R. Bates, K. Ledsham, and A. L. Stewart, *Philos. Trans. R. Soc. London, Ser. A* **246**, 215 (1954).
- [6] A. López-Castillo, *Phys. Rev. Lett.* **77**, 4516 (1996).
- [7] J. Müller, J. Burgdörfer, and D. W. Noid, *J. Chem. Phys.* **103**, 4985 (1995).
- [8] Y. Duan, J.-M. Yuan, and C. Bao, *Phys. Rev. A* **52**, 3497 (1995).
- [9] D. Wintgen, K. Richter, and G. Tanner, *Chaos* **2**, 19 (1992).
- [10] A. López-Castillo, M. A. M. de Aguiar, and A. M. Ozorio de Almeida, *J. Phys. B* **29**, 197 (1996).
- [11] P. V. Coveney and M. S. Child, *J. Phys. B* **17**, 319 (1984).
- [12] H. A. Erikson and E. L. Hill, *Phys. Rev.* **75**, 29 (1949).
- [13] E. L. Stiefel and G. Scheifele, *Linear and Regular Celestial Mechanics* (Springer-Verlag, Berlin, 1971).
- [14] M. Baranger and K. T. R. Davies, *Ann. Phys. (N.Y.)* **177**, 330 (1987).
- [15] J. H. van Vleck, *Philos. Mag.* **44**, 842 (1922).
- [16] J. G. Leopold and I. C. Percival, *J. Phys. B* **13**, 1037 (1980).
- [17] J.-M. Richard, *Phys. Rev. A* **49**, 3573 (1994).
- [18] V. N. Ostrovsky and N. V. Prudov, *J. Phys. B* **30**, 151 (1997).
- [19] G. S. Ezra, K. Richter, G. Tanner, and D. Wintgen, *J. Phys. B* **24**, L413 (1991).
- [20] J. H. Eberly, *Phys. Rev. A* **42**, 5750 (1990).
- [21] T. Ménis, R. Taïeb, V. Véniard, and A. Maquet, *J. Phys. B* **25**, L263 (1992).
- [22] D. Wintgen, *Phys. Rev. Lett.* **61**, 1803 (1988); J. M. Robbins, *Nonlinearity* **4**, 343 (1991).
- [23] The MELD codes were developed by E. R. Davidson, L. E. Murchie, S. T. Elbert, and S. R. Langhoff with extensive modifications by D. Rawlings and D. Feller; E. R. Davidson, in *Modern Techniques in Computational Chemistry: MOTTEC-91*, edited by E. Clementi (Escom, Leiden, 1991), p. 381.
- [24] I. Shimamura, C. J. Noble, and P. G. Burke, *Phys. Rev. A* **41**, 3545 (1990).
- [25] S. L. Guberman, *J. Chem. Phys.* **78**, 1404 (1983).
- [26] H. Takagi and H. Nakamura, *Phys. Rev. A* **27**, 691 (1983).
- [27] J. G. Leopold, I. C. Percival, and A. S. Tworkowski, *J. Phys. B* **13**, 1025 (1980).
- [28] Y. Sugiura, *Z. Phys.* **45**, 484 (1927).
- [29] K. Richter, J. S. Briggs, D. Wintgen, and E. A. Solov'ev, *J. Phys. B* **25**, 3929 (1992).
- [30] C. W. Bauschlicher, Jr. and M. Rosi, *Chem. Phys. Lett.* **159**, 485 (1989); M. Kolbuszewski and J. S. Wright, *Can. J. Chem.* **71**, 1562 (1993); P. C. Cosby, R. Möller, and H. Helm, *Phys. Rev. A* **28**, 766 (1983).